Impairment of T cells' antiviral and anti-inflammation immunities dominates the death from COVID-19

Luhao Zhang[1,2†], Rong Li[1,3†], Gang Song[4], Gregory D. Scholes[2*] and Zhen-Su She[1,3*]
[1]Institute of Health System Engineering, College of Engineering, Peking University, Beijing, China, 100871.
[2]Department of Chemistry, Princeton University, Princeton, NJ, 08540.
[3]State Key Laboratory for Turbulence and Complex Systems, Peking University, Beijing, China， 100871.
[4]Beijing Hospital, National Center of Gerontology; Institute of Geriatric Medicine, Chinese Academy of Medical Sciences, Beijing, China, 100730
†These authors contribute equally
[*]Corresponding author: Gregory D. Scholes, 609-258-0729, gscholes@princeton.edu, 125, Frick Laboratory, Department of Chemistry, Princeton University, Princeton, NJ, and Zhen-Su She, 010-62766559, she@pku.edu.cn, 206, Peking University State Key Laboratory of Turbulence and Complex Systems, Beijing, China.

Author Contributions: L.Z., G.S. and R.L. performed research; Z.S. and R.L. designed research; L.Z, R.L., Z.S., G.S., G.D.S. wrote the paper; Z.S. supervised the project; G.D.S funded the project

Competing Interest Statement: The authors declare no competing interests

Keywords: COVID-19, immunology and inflammation, mathematical model, T cell

Abstract

Clarifying key factors dominating the immune heterogeneity from non-survivors to survivors is crucial for therapeutics and vaccine developments against COVID-19. The main difficulty is to quantitatively analyze the multi-level clinical data of viral dynamics, immune response, and tissue damages. Here, we adopt top-down modeling to quantify key functional aspects and their dynamical interplays in the virus-immune system battle, yielding an accurate description of real-time clinical data involving hundreds of patients for the first time. The quantification of antiviral responses demonstrates T cells' dominant role in the virus clearance relative to antibodies, especially for mild patients (96.5%). Moreover, the anti-inflammatory responses, namely cytokine inhibition rate and tissue repair rate also have positive correlations with T cell number, and are significantly suppressed in non-survivors. Simulations show that impaired immune functions of T cells leads to greater inflammation (thus dominates the death), explaining the monotonous increase of COVID-19 mortality with age and higher mortality for males. We conclude that T cells play the role of crucial immunity that saves the death from COVID-19, which points out a new direction to advance current prevention and treatment by incorporating the vaccines, drugs and health care activities that aim to improve T cells' number and functions.

Introduction

The ongoing COVID-19 pandemic has resulted in over two million deaths worldwide. Therefore, identifying key factors that determine the immune heterogeneity from non-survivors to survivors is crucial for the current fight against the pandemic. Past clinical study has found a series of host factors associated with severe disease or higher mortality via correlation analysis: individual characteristics including older age, male sex, and comorbidities[1,2]; profound lymphopenia, with T cells most significantly affected[3–5]; the elevated level of inflammation markers, like LDH (lactate dehydrogenase) and D-dimer[2,6]; excessive release of pro-inflammatory signaling molecules, like IFN − γ, IL-6, etc., known as the cytokine storm which is thought likely to be a major cause of multiorgan failure[4,7]. For immune responses, both SARS-CoV-2 specific T cells and antibodies are observed in COVID-19 patients[6,8]. However, the quantitative role of these factors in antiviral and anti-inflammatory immune responses is unknown, resulting in several unsolved questions about the cause and saving of the death: 1. What is the relative importance of T cell and antibody response for antiviral immunity at different stages; 2. What are the main driver and suppressors for the cytokine storm and multiorgan failure? And most importantly, 3.Are there new directions to overcome the heterogeneity of patients, decay of antibody function, and gene mutation of SARS-CoV-2 in efficient therapeutics and vaccine developments?

Beyond correlative analyses, quantitative modeling is a powerful tool to simulate the measured dynamical immune response to reveal the relative importance of different components[9]. However, most recent studies focus on the simple viral dynamics and its interactions with immune responses[10,11]and antiviral drugs[12–21], without considerations of organ damages and disease progression. On the other hand, some multiscale simulations [22–24] incorporate existing knowledge about the viral dynamics, immune responses, and comorbidities to simulate the clinical outcomes. However, these approaches involve hundreds of model parameters, which have considerable value uncertainties that limit the reliability of predictions and systematic comparisons with clinical data. Therefore, previous studies are either oversimplified or overcomplicated to clarify the key factors dominating death.

In this work, we adopt a top-down modeling to quantify crucial aspects in the virus-immune system battle to overcome this difficulty. Here, the battle is classified into three kinds of functional behaviors, namely, the pathogenic functions (e.g., virus and inflammation), the protective functions (e.g., innate and adaptive immunity), and the organ damages. Integrating with the existing clinical and immunological knowledge for COVID-19 patients, we establish a dynamical motif for a small set of crucial functional variables and their interplays. This antiviral-inflammation model is used to simulate the systematic progression of COVID-19 patient with 19 measurable parameters. These simulations are validated with real-time clinical data involving hundreds of patients and then used to evaluate contributions of T cells and antibodies to antiviral immune responses. Subsequently, we quantify the difference of anti-inflammatory immune responses from non-survivors to survivors and clarify their correlations to T cells. Finally, T cells' dominant role in saving the death of COVID-19 and revelation to new therapeutics and vaccine development are discussed.

Causal network of the Antiviral-Inflammation Model

The difficulty of previous multiscale simulations[22–24] due to considerable parameter value uncertainties stems from the fact that, in the bottom-up strategy, the immune response to infectious disease is modeled as a complex network of numerous factors, resulting in the so-called 'curse of dimensionality'[25]. In contrast, a recent successful model of a classical complex system, namely, fluid turbulence, one of us has demonstrated that the global motions composed of numerous components typically display a symmetry-breaking which can be quantitatively modeled with finite functional variables, called order functions[26,27]. Here, we use a similar top-down strategy to quantify immune functional aspects in the virus-immune system battle.

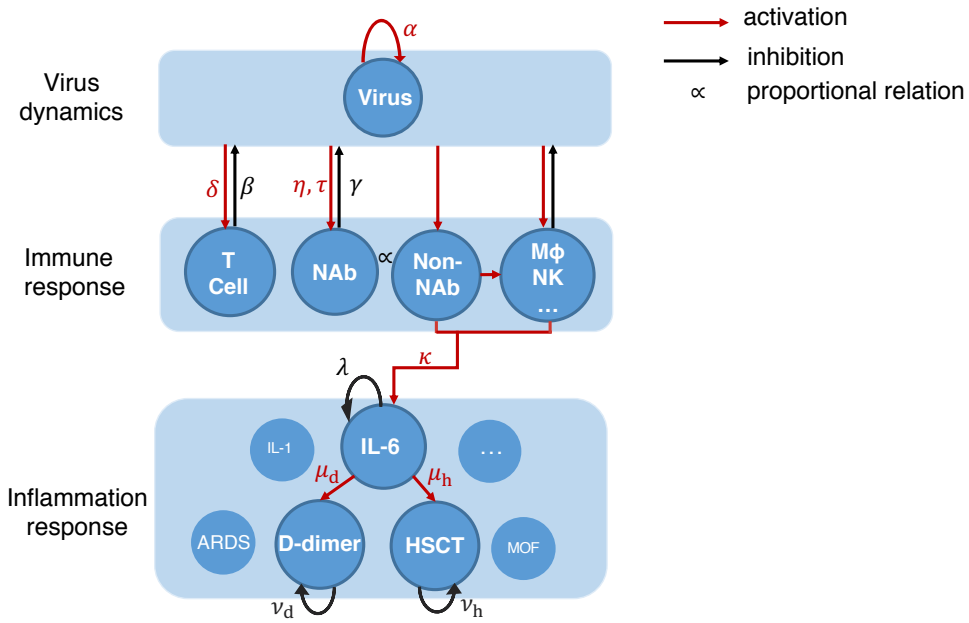

Figure 1. Graphical scheme of COVID-19 antiviral-inflammation model. Key components are highlighted. The red arrows mean activation, and the black arrows mean inhibition. Greek letters mean the activation/inhibition rates or characteristic time associated with each interactionNAb: neutralizing antibody. Non-NAb: non-neutralizing antibody. Mϕ, NK: macrophage and natural killer cells. IL-6: interleukin 6. IL-1: interleukin 1. D-dimer: coagulation marker. HSCT: High-sensitivity cardiac troponin I, heart injury marker. ARDS: Acute Respiratory Distress Syndrome. MOF: Multi-Organ Failure.

The model explicitly describes dynamics of five crucial functional quantities that determine COVID-19 progression: virus and interleukin 6 (IL-6) for pathogenic function, effector T cells and neutralizing antibodies for protective function, D-dimer (coagulation marker), and high-sensitivity cardiac troponin I (HSTC, heart injury marker) as examples for multi-organ damage. Other secondary factors modulate their interactions. Fig.1 shows their interplay following time order from virus dynamics, immune response to inflammation response. Self-replicating virus stimulates innate and adaptive immune cells which can produce antibodies. Effector T cells and neutralizing antibodies (NAbs) clear virus directly, either by killing infected cells or block the virus from entering into tissue cells; non-neutralizing antibodies (Non-NAbs) combines with innate immune cells (macrophages (Mϕ) and nature killers (NK), etc.) and induce immunoreaction to clear virus indirectly. The activated immune cells secrets cytokines, in which IL-6 has a central role for downstream destructive effect on organs, hence, it increases D-dimer and high-sensitivity cardiac troponin I that characterizes multiorgan failure (MOF). On the other hand, suppressing immune hyperactivation and tissue repair by negative feedback

reduces activated immune cells and vessel and heart damage, thus reducing IL-6, D-dimer, and high-sensitivity cardiac troponin I.

Mathematical description of the Antiviral-Inflammation Model

Quantitatively, a set of ordinary differential equations, (1)-(5) is constructed to describe the antiviral immune response and pathogenesis of inflammation at a specific part of the body. The detailed meanings and units of all parameters are provided in SI (Supplementary Information), Table S1. The antiviral process includes continuous virial replication, dynamical activation of T cells to effector T cells by the virus, dynamical secretion of neutralizing antibodies by B cells, virus clearance by effector T cells and antibodies, and decay of effector T cells and antibodies. Eq. (1)-(3) describes the corresponding dynamical evolutions of concentrations of the virus, effector T cells, and neutralizing antibodies, with concise rate constants and time interval describing global effects of a series of microscopic processes, like target cell infection, antigen identification, antigen presentation, differentiation of T cells, B cell immunoglobulin class switching, etc. The antiviral effect of innate immunity is absorbed into an effective viral replication rate, $\tilde{\alpha}$. Eq. (4) shows that the release of IL-6 is proportional to concentrations of non-neutralizing antibodies (assumed to be proportional to neutralizing antibodies) which combine with innate immune cells and trigger pro-inflammatory pathways. Immune suppressing reduces activated immune cells and, therefore, the IL-6 level. The release of IL-6 causes damage to organs, like thrombus formation and heart injury marked by D-dimer and high-sensitivity cardiac troponin I, whose levels are reduced when blood vessels and heart are repaired, shown in Eq. (5).

$$\frac{dV(t)}{dt} = [\tilde{\alpha} - \beta T_{\mathrm{e}}(t) \ - \gamma[A(t) - A_0]]V(t) \tag{1}$$

$$\frac{dT_{\mathrm{e}}(t)}{dt} = \delta V(t) - \epsilon T_{\mathrm{e}}(t) \tag{2}$$

$$\frac{dA(t)}{dt} = \eta V(t-\tau) - \theta[A(t) - A_0](t) \tag{3}$$

$$\frac{dI(t)}{dt} = \kappa A(t) - \lambda[I(t) - I_0] \tag{4}$$

$$\frac{dS_i(t)}{dt} = \mu_i I(t) - \nu_i S_i(t) \tag{5}$$

Simulations of Eq. (1)-(5) are compared to real-time data with 457 patients involved. Ten are individuals, and 447 patients form mild, severe, survivor, and non-survivor groups

whose median data are compared. For detailed data sources and integration of data from different sources, see Methods and SI. The time axis for simulation is the number of days after symptom onset, with the starting day being 0 or several days earlier. The numerical simulation is propagated using the delayed differential equations (DDE) of MATLAB. The least-square fit is achieved using the *fmincon* function of MATLAB with the implemented interior-point optimization algorithm. For a detailed description of fitting procedure and parameter uncertainty estimation, see Methods and SI.

Results

Viral dynamics and contributions of T cells and antibodies to antiviral responses

Virus, effector T cell, and antibody dynamics are simulated and compared with real-time data from 10 individuals[28,29] and median values of mild and severe (critical) groups, survivors, and non-survivors[30–32]. The concentrations of virus (V), effector T cells (T_e), and antibodies (A) is assumed proportional to viral load measurement from the respiratory tract, the change of T cells (T) from its baseline level (T_0) measured in peripheral blood ($T_0 - T$), and optical density or titer of Anti-RBD IgG/Anti-S1 IgG/Anti-NP IgG, respectively. CD3+ T cell (all T cells) data from cases of the same severity compensate for those who lack CD3+ T cell data. Original lymphocyte count is scaled by 0.589(Methods) for T cell count. As shown in Fig.2 and Supplementary Fig.1, simulations show agreement to data for all cases; for parameters, see SI.

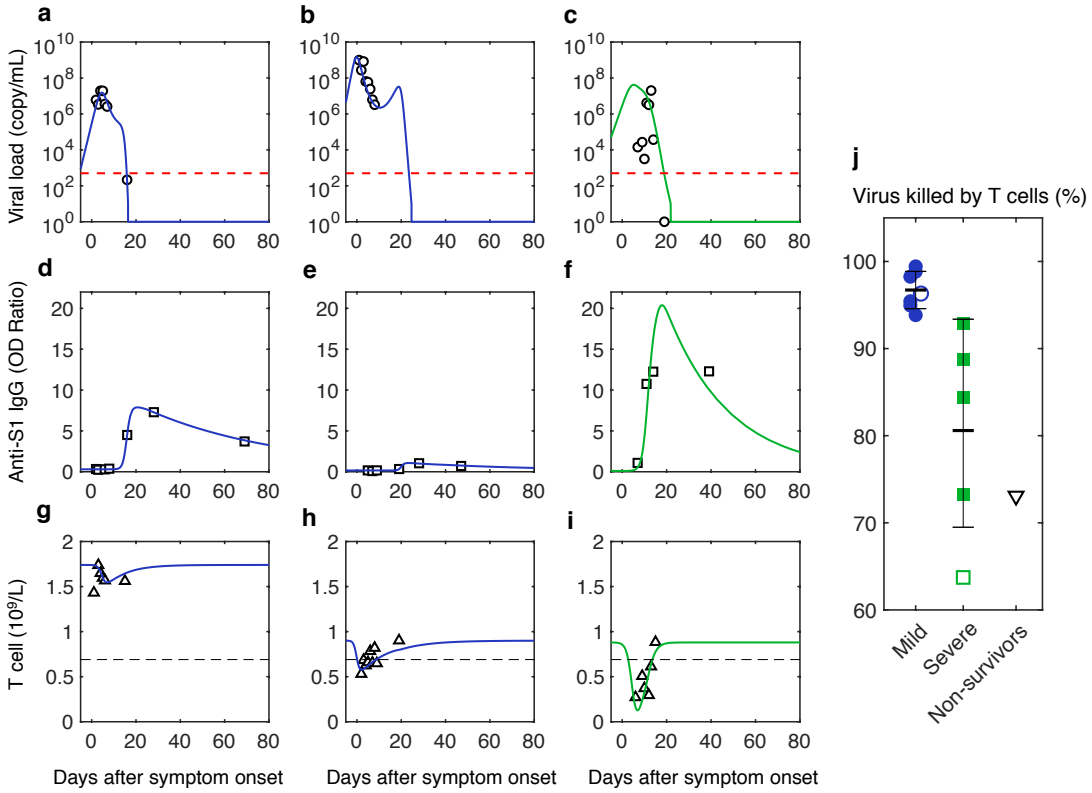

Figure 2. Viral dynamics, adaptive immune response, and contributions of T cells to antiviral responses. a, d, g are of patient P1, b, e, h are of patient P2, c, f, i are of patient P3[28]. Mild patients are in the blue and severe patient is in green. Red dotted lines are the limit of detection. Black dotted lines are normal ranges. Viral load is from the nasopharyngeal swab. For fitted parameters and the other 10 cases, see SI Table S4. j: An overall statistic of the fraction of virus killed by T cells for all cases shows T cells' contribution is significantly higher in mild patients than severe patients. Solid markers are individual data and hollow markers are group data. Error bars represent standard errors.

Clarifying deterministic factor controlling viral load peak benefits early antiviral treatment, vaccination, and epidemiological control[33]. By asymptotic analysis (Methods), the model predicts the peak is determined from virus inhibition by T cells: peak value is the ratio between square of virus replication rate and two times the multiplication of T cell activation and virus clearance rate. This gives 1.37×10^7 copy/mL for the viral peak of patient P1 in Fig.2. Data agreement gives that for patients who survive, on average, 95% of viruses are cleared per day with 10^9/L T cells from blood engaged, revealing strong efficiency of T cells' virus clearance. In conclusion, the consistency between simulation and data clarifies the antiviral dynamics for various severities in which adaptive response plays a significant role---first, effector T cells are activated, kill

infected cells, and induce viral peak; then neutralizing antibodies are secreted, finally clear the virus.

To clarify the roles of T cells and antibodies in the antiviral process, we define the amount of virus cleared by T cells, N_{T} and antibodies, N_{A}, are: $N_{\mathrm{T}}(t) = \int_{\mathrm{N}}^{t} \beta T(t')V(t')\,dt'$ and $N_{\mathrm{A}}(t) = \int_{\mathrm{N}}^{t} \gamma[A(t') - A_0]V(t')\,dt'$. Then, the contribution by T cells for clearing the detectable virus, F_{T} and contribution of antibodies, F_{A}, are: $F_{\mathrm{T}} = \int N_{\mathrm{T}}(t)dt/[\int [N_{\mathrm{T}}(t) + N_{\mathrm{A}}(t)]dt]$, $F_{\mathrm{A}} = 1 - F_{\mathrm{T}}$.

For patients of different severities, we compare the quantitative contributions of T cells and neutralizing antibodies for virus clearance as displayed in Fig.2j. It shows T-cell immunity dominates the total virus clearance for all patients (88.8%) but significantly decreases from mild to severe patients, consistent with previously reported less CD4+, CD8+ response in severe patients compared to mild patients[8]. Instead, the antibodies' contributions are 3.3% (mild), 19.4% (severe or critical) and 28.9% (non-survivors), respectively. Our simulation finds that the antibody preparation time before secretion is overall smaller in severe cases (9.42, 5.40-12.79 day) than in mild cases (14.68, 8.45-20.13 day), revealing antibodies in severe patients secrete earlier and cleared more virus. In conclusion, we demonstrate in COVID-19 that T cells have a dominant role in the virus clearance relative to antibodies, especially for mild patients.

Inflammation dynamics associated with death

To clarify the main driver for the cytokine storm and organ damage of critical illness, we compare simulations of Eq. (4)-(5) with real-time, median data of survivors and non-survivors (Fig.4). The concentration of non-neutralizing antibodies is assumed proportional to anti-RBD IgG optical density. For data source and parameter estimation, see Methods and SI. The agreement between simulations and data of IL-6, D-dimer, and high sensitive cardiac troponin I proves non-neutralizing antibodies stimulate the secretion of IL-6, and IL-6 stimulates the accumulation of D-dimer and high sensitive cardiac troponin I. IL-6 formation rates are assumed to be the same for both groups. The striking feature of non-survivors compared to survivors is the continuous production of IL-6 and organ damage, revealed by zero inhibition rates for all three markers (Fig.4b), while the difference of formation rates of organ damage markers is not remarkable.

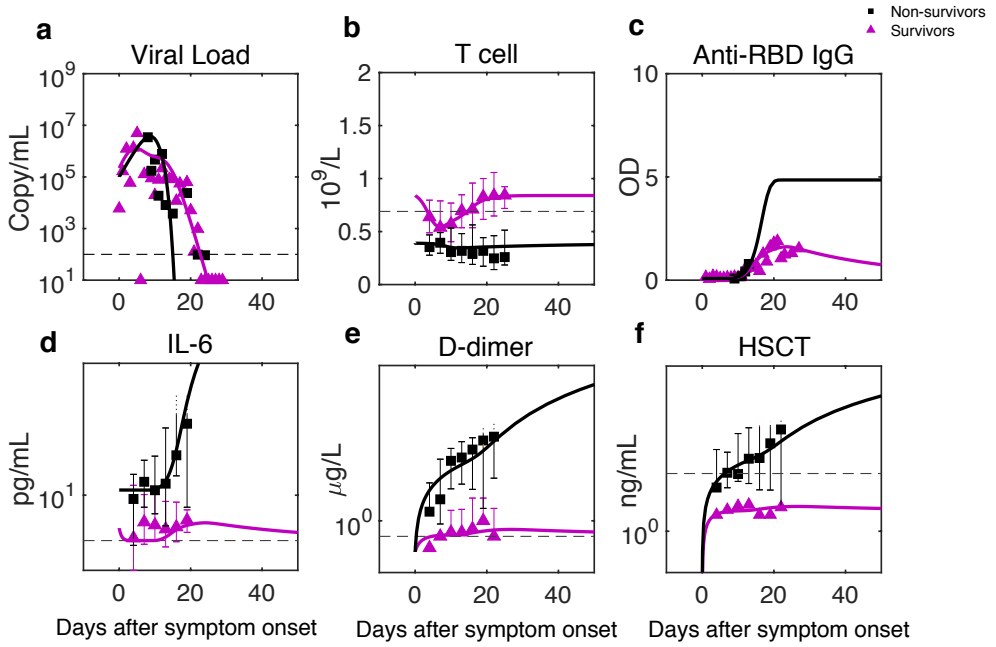

Figure 3. Comparison of predictions to clinical data of survivors and non-survivors reveals the mechanism for death from COVID-19. The data are the median of the group with error bars from reference[32]. The IL-6, D-dimer, and elevated sensitive cardiac troponin I inhibition rates are all zero for non-survivors, which gives continuous deterioration in contrast to non-zero inhibition rates of survivors who recover. For parameter estimation, see Methods and SI. The saturation value of Anti-RBD IgG for non-survivors is estimated by assuming its ratio to the maximum of survivors'(18 non-critical and three critical) data is close to the ratio of maximums of neutralizing antibodies between critical and non-critical patients[34].

We conclude that the main trigger of cytokine storm is the secretion of elevated non-neutralizing antibodies which combine with innate immune cells and activate cytokine release pathways; the lack of negative feedback for immune suppression in non-survivors makes cytokine keeps accumulating. The cytokines act as the primary source that causes damage to organs, and the lack of tissue repair in non-survivors continues to worsen the illness. Our finding reveals the crucial aspect of death from COVID-19 is the lack of negative feedback for anti-inflammatory cytokine inhibition and tissue repair.

Initial T cells as background immunity that reduce mortality

Our model reveals that T cells' virus clearance, cytokine inhibition, and tissue repair are three essential protective functions in COVID-19 that determine disease severity. To seek what determines these protective functions, T cells' contribution of total virus clearance, cytokine inhibition rate, and tissue repair rates are plotted with initial T cell concentration before infection (equal to T cell baseline, T_0) in Fig.4.a,b, which shows a positive

correlation (Fig. b is based on statistics of 137 non-survivors and 54 survivors). It shows the importance of sufficient initial T cells for comprehensive protection, which comes from an adequate number of effective CD8+ effector T cells that kill infected cells, sufficient regulatory T cells and other subsets that suppress the immune response and promote tissue repair[35] to reduce over inflammation in non-survivors.

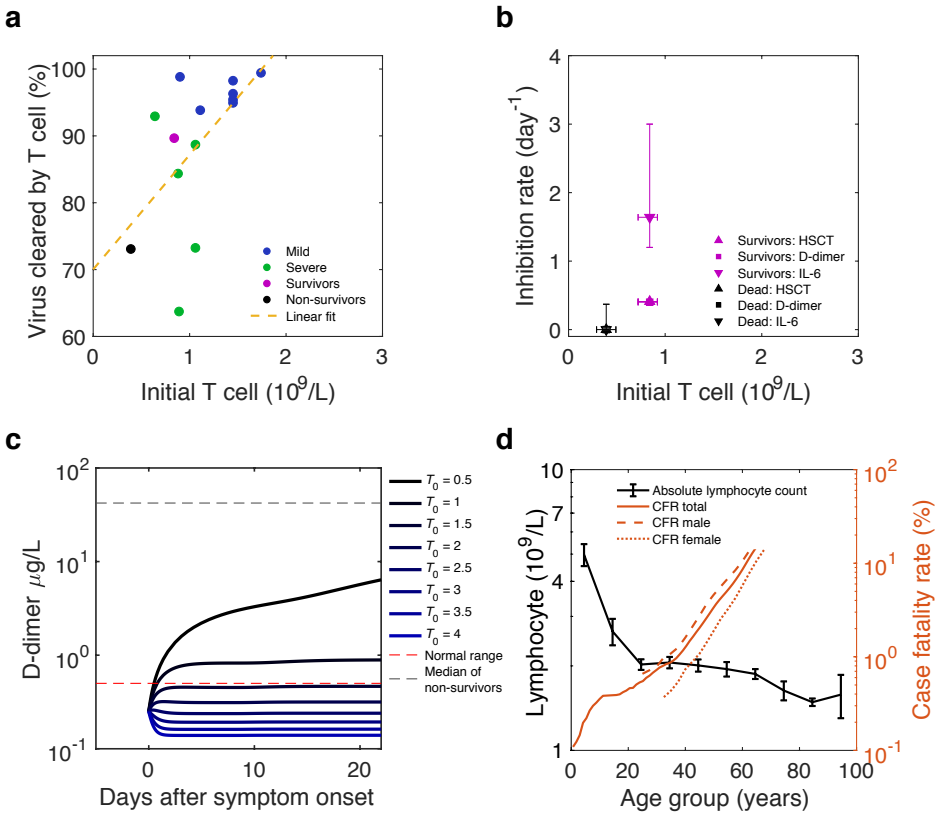

Figure 4. Initial T cell concentration as the background immunity of individuals against SARS-CoV-2 and reduces mortality. a and b: T cell's antiviral contribution, IL-6, D-dimer and high sensitive cardiac troponin (HSCT) inhibition rates are positively correlated with initial T cell concentration. c: D-dimer dynamics of non-survivors with increase of initial T cell concentration (T_0) reduces organ damage at late stage. The Red dashed line is the normal upper limit of the D-dimer, and the grey dashed line is the median value of the non-survivor group from reference[32]. For parameters of simulation, see Methods. d. Lymphocyte count decreases with age and mortality(case fatality rate, CFR) increases with age. Male (dashed line) have higher mortality than female (solid line).

A great public concern is how an individual patient's background 'immune health' landscape (simplified as background immunity) shapes responses to SARS-CoV-2 infection[36] and controls the disease's severity. Because of the determining relation of initial T cell concentration for protective functions, T cells' static reserve before infection and dominance in population compared to other cells against the virus, we propose

concentration of initial T cells is a crucial characterization for the background immunity against SARS-CoV-2. To verify this hypothesis, we conduct disease progression of patients with different initial T cell concentrations. According to Fig.4 a,b, by assuming a linear decreasing of T cells' virus clearing rate, IL-6 and D-dimer inhibition rates with decreasing initial T cell concentration, Fig. 4c shows coagulation becomes more and more significant, which means lack of initial T cells exacerbates disease severity and increase mortality risk.

Therefore, we conclude that the T cells' impaired antiviral and anti-inflammation functions are the main immune origin of death from COVID-19: the extremely low level of initial T cells in non-survivors results in weak antiviral, cytokine inhibition and tissue repair abilities as well as low tissue repair function; then it calls the elevated antibodies for compensation; as a result, the concomitant large amount of non-neutralizing antibodies amplifies the cytokine storm, leading to continued damage. Following this casual chain, according to the decrease of lymphocytes (hence decrease of T cells assuming T cell count proportional to lymphocyte count) with older age (Fig.4d), we predict straightforwardly older patients must have higher mortality than younger patients. Also, male patients should have higher mortality than female patients for their lower level of CD4+ T cells[37]. Our prediction explains the continuous increase of COVID-19 mortality with age and higher mortality for males[37], shown in Fig. 4d.

Discussion

In conclusion, we have quantified the adaptive-immune-response heterogeneity from non-survivors to survivors of COVID-19, using a dynamical motif with 19 measurable parameters beyond the overcomplication of the previous multiscale model[24]. For the first time, this model provides an accurate description of real-time clinical data involving hundreds of patients, which then reliably clarifies T cells' dominant roles in the antiviral and anti-inflammatory immune responses. Beyond the previous correlation analysis for T cell scarcity and disease severity[8,36], this work reveals the causal relation between death from COVID-19 and impaired T cell immunity. This discovery explains the high mortality of older man and points out a new direction for therapeutics and vaccine development.

The currently tested drugs target various pathogenesis levels, from antiviral to anti-inflammatory drugs and antithrombotic agents[24], etc. However, there is no proven effective therapeutics for COVID-19. One crucial challenge is the lack of broad applicability of these drugs to heterogeneous patients with various comorbidities, disease severities, and complications[38]. Our study points out a new direction will be increasing T cell number and functions by both drugs and health care activities, which may benefit

virus clearance, cytokine inhibition, and tissue repair simultaneously. Firstly, recent studies reported the curing effect of drugs to COVID-19 patients by increasing T cell number, e.g., recombinant human granulocyte colony-stimulating factor[39] JinHuaQingGanKeLi[40]. Therefore, we encourage further studies and applications in this direction. Second, for the recovery of COVID-19 patients and healthy people's prevention, improving background immunity associated with T cells is more important and promising. Therefore, we strongly suggest studying the curing and immunity improvement effects of health care activities, such as mediation[41,42], Tai Chi[43] and BaDuanJin[44], for previous studies have found they help to increase CD3+ T cell and CD4+ T cell concentration and apply to a wide range of age, including older adults.

On the other hand, in the current development of the vaccine, neutralizing antibody immunity plays a crucial role. Unfortunately, the single-strand RNA structure makes SARS-CoV-2 easy to mutate, and several lineages have been discovered[45]. These mutations pose challenge for long-term effectiveness of antibody immunity, for it is on the molecular level targeting specific epitopes of the virus. By contrast, memory T cells show strong cross-reactivity and persistence[46], and active T cells protect bodies in several aspects, including antivirus, suppress immune hyperactivation, and promote tissue repair. Therefore, stimulation of T cell response by the vaccine is worth more exploration, and we suggest advancing the current combination adjuvant strategy[47] that elicits potent CD8 and CD4 T cell responses.

For clinical application, to maximize the curing effect for severe patients, we suggest adopting multistage, synthetic protocols incorporating the above therapies. In this case, our model provides a strong tool to evaluate the effectiveness of treatments to identify individual optimal protocols. The reason is that all parameters can be determined from clinical data and quickly predict individual patients' trajectories, which may also advance the early prediction algorithm of current artificial intelligence softwares[48,49].

To separate the critical elements from irrelevant details, we here have made some assumptions, which should be evaluated in further clinical studies, although they would not affect the basic conclusions of the study. For instance, the virus-clearance rate of innate immunity is thought to be a constant with negligible variation and is small compared to rates of adaptive response, which should be verified by further time-dependent measurement of the course of innate response. The second assumption that needs more measurement to test is that, for survivors, the concentration of effector CD8+ T cells at the infected part is proportional to the reduction of CD3+ T cells in peripheral blood; whether it is strictly obeyed at the most time or not might be intriguing to further investigation[4]. The third questionable assumption is that the temporal profile of non-

neutralizing antibodies is proportional to neutralizing antibodies. Further measurement needs to test whether they are secreting at the same pace or not.

Methods

- **Asymptotic analysis of viral load peak**

Around the viral load peak, with the decay of effector T cells and the production of antibodies neglected, the evolutions of viral load and effector T cells become:

$$\frac{dV(t)}{dt} = [\tilde{\alpha} - \beta T_{\mathrm{e}}(t)\,]V(t) \tag{6}$$

$$\frac{dT_{\mathrm{e}}(t)}{dt} = \delta V(t) \tag{7}$$

The analytical solutions are:

$$V(t) = V^* \frac{4}{2 + e^{-\tilde{\alpha}(t-t^*)} + e^{\tilde{\alpha}(t-t^*)}}, V^* = \frac{\tilde{\alpha}^2}{2\beta\delta} \tag{8}$$

$$T_{\mathrm{e}}(t) = 2\tilde{\alpha} \frac{1}{1 + e^{-\tilde{\alpha}(t-t^*)}} \tag{9}$$

where V^* is viral load peak described in the first section of Results, and t^* is the corresponding time.

- **Extraction of data from published literature**

A software tool WebPlotDigitizer (https://automeris.io/WebPlotDigitizer) was used to extract data from fig.2 in ref[3], fig.1 and fig.3 in ref[28], fig.2 in ref[2], fig.1 and fig.3 in ref[30] and fig.3 in ref[31]. All extracted data were made available to readers in our GitHub shared folder: https://github.com/luhaozhang/covid19

- **Integration of data from different sources**

The data we used here contains 10 individuals and 4 groups. Individuals contain 6 mild and 4 severe (including critical) patients. The CD3+ T cell data of mild, severe and critical population from Hongzhou Lu[3]'s cohort were used for individual patients and groups of the same severity who don't have T cell data. 4 patients were from Isabella Eckerle's[1] cohort and 6 patients from Kelvin To's[2] cohort, and the severity classification follows the assignments in previous publications. One patient from Kelvin To's cohort who have not yet been identified as being critically ill is classified as severe because the probability of being critically ill is low (1/6). For mild, severe (including critical) and non-survivor groups, Table S2 lists the sources of virus, T cells, and antibodies. T cells, IL-6, D-dimer and HSCT were from BinCao's cohort[32] for both survivors (137 patients) and non-survivors (54 patients). Virus and Anti-RBD IgG for survivors

were from the median of 20 survivors from Kelvin's cohort[50]. Lymphocyte data were multiplied by 0.589 to get estimated T cell concentration (0.589 is the ratio between medians of normal ranges of T cells[3] and lymphocytes[28])

- **Least square fit of virus, immune response and inflammation data**

For parameters of simulations in Fig.2 and Fig.4, we adopt a best-fit approach to find the parameters which minimize the given objective function: the mean of residual sum of squares (RSM) between data points and the corresponding model simulations as used similarly in influenza model[51]. For virus-T cell-antibody dynamics, the objective function is:

$$\overline{RSM} = \frac{1}{n_V}\sum_{i=1}^{n_V}\left[\frac{(\log 10\, V_i - \log 10\, \bar{V}_i)}{\log 10\, V_{max}}\right]^2 + \frac{1}{n_T}\sum_{i=1}^{n_T}\left[\frac{(T_i - \bar{T}_i)}{T_{max}}\right]^2 + \frac{1}{n_A}\sum_{i=1}^{n_A}\left[\frac{(A_i - \bar{A}_i)}{A_{max}}\right]^2 \quad (10)$$

V_i is viral load data, $\bar{V}_i$ is the value given by model, n_V is the total number of data points. The instructions are similar for T cells(T) and antibodies(A). For the objective function of inflammation response, mean of RSM (Eq. (11)) was used in linear scale for survivors and log scale (Eq. (12)) for non-survivors:

$$\overline{RSM} = \frac{1}{n_I}\sum_{i=1}^{n_I}\left[\frac{(I_i - \bar{I}_i)}{I_{max}}\right]^2 + \frac{1}{n_{S_\mathrm{d}}}\sum_{i=1}^{n_{S_\mathrm{d}}}\left[\frac{(S_{\mathrm{d}i} - \overline{S_{\mathrm{d}i}})}{S_{\mathrm{d}max}}\right]^2 + \frac{1}{n_{S_\mathrm{h}}}\sum_{i=1}^{n_A}\left[\frac{(S_{\mathrm{h}i} - \overline{S_{\mathrm{h}i}})}{S_{\mathrm{h}max}}\right]^2 \quad (11)$$

$$\overline{RSM} = \frac{1}{n_I}\sum_{i=1}^{n_I}\left[\frac{(\log 10\, I_i - \log 10\, \bar{I}_i)}{\log 10\, I_{max}}\right]^2 + \frac{1}{n_{S_\mathrm{d}}}\sum_{i=1}^{n_{S_\mathrm{d}}}\left[\frac{(\log 10\, S_{\mathrm{d}i} - \log 10\, \overline{S_{\mathrm{d}i}})}{\log 10\, S_{\mathrm{d}max}}\right]^2 + \frac{1}{n_{S_\mathrm{h}}}\sum_{i=1}^{n_A}\left[\frac{(\log 10 S_{\mathrm{h}i} - \log 10 \overline{S_{\mathrm{h}i}})}{\log 10 S_{\mathrm{h}max}}\right]^2 \quad (12)$$

For simulation of viral load dynamics, when V<10 copy/mL, it is thought to be cleared thoroughly at one time without further evolution and is set to be 1 copy/mL. Table S3 lists the data points used for performing the best fit of each case. Viral data points that represent negative results of virus were abandoned unless they were important indicators of the ending of viral activity. The viral data points associated with the second viral load peak in mild and severe group were not used for any fits because the phenomenon is not observed as the common feature of individual patients. The decay of CD3+ T cells of 902 and 910 patients after 30 days were not used for fit at present. The decay was attributed as a deviation from averaged behavior on group level because of the large 95% CI of the data.

When performing best fit related with I, S_d, and S_h, parameters of virus, T cells and antibodies had been fixed. Estimation of uncertainty of parameters is carried out by performing a series of fits after the best fit for each case. For uncertainties of $\kappa, \lambda, \mu_\mathrm{d}, \nu_\mathrm{d}, \mu_\mathrm{h}, \nu_\mathrm{h}$, as shown in Fig.4, a set of fits was performed, each time by varying one data point of IL-6, D-dimer or HSCT to its upper or lower limit. The uncertainties for each fitted parameter were estimated as the minimum and maximum of each parameter among all fits. The best fits and uncertainties were summarized in Table S5. 95%CI is not used for uncertainty here because the number of data points is small. For methods and results of uncertainties of antiviral parameters, see SI.

fmincon function of MATLAB (MathWorks, version 2012 and higher) with the implemented interior point optimization algorithm was used to perform the fits. It requires constraints for the parameters to be optimized and an initial guess. An empirical fitting is performed for each patient and group to identify ranges of parameters' constraints for optimization, shown in Table S6 and Table S8. Patients with the same type of data and same severity category are set to have similar ranges. Table S7 and Table S8 show the empirical values of parameters as initial guesses for best fits. Random initial guess is not suitable here because the fit is sensitive to the initial space, probably because of the limited number of data points with relatively large fluctuation, especially for viral load. For instructions about fixed parameters during the fitting, see SI. Parameters of best fits were used as initial guesses of fits when estimating parameters uncertainties.

- **Simulation of D-dimer dynamics with different initial T cell concentration**

Based on the positive correlation of T cell antiviral contribution, IL-6 and D-dimer inhibition rates, we assume a linear increase of T cell activation rate, δ and inflammation inhibition rates, λ, ν_d, ν_h with initial T cell concentration T_0 as shown in the eq.(13)-(16). When T_0 takes value of survivors' and non-survivors' median as in Fig.3(b), the parameters equal to their fitted values. Simulation in Fig.4(c) is performed using a series of given T_0, the corresponding δ, λ, ν_d, ν_h and all other parameters of non-survivor group and their values remain unchanged.

$$\delta = 0.25 + 21.67 \times (T_0 - 0.39) \quad (13)$$

$$\lambda = 3.64 \times (T_0 - 0.39) \quad (14)$$

$$\nu_d = 0.889 \times (T_0 - 0.39) \quad (15)$$

$$\nu_h = 0.911 \times (T_0 - 0.39) \quad (16)$$

Acknowledgments

The research is funded by the W.M. Keck Foundation through award no. 1005586. The authors acknowledge Prof. Kelvin To for sharing data, and Xiaoquan Wang, Guanghui She for discussion.

References

1. Docherty, A. B. *et al.* Features of 20 133 UK patients in hospital with covid-19 using the ISARIC WHO Clinical Characterisation Protocol: prospective observational cohort study. *BMJ* **369**, m1985 (2020).

2. Zhou, F. *et al.* Clinical course and risk factors for mortality of adult inpatients with COVID-19 in Wuhan, China: a retrospective cohort study. *Lancet* **395**, 1054–1062 (2020).

3. Zhang, X. *et al.* Viral and host factors related to the clinical outcome of COVID-19. *Nature* **583**, 437–440 (2020).

4. Merad, M. & Martin, J. C. Pathological inflammation in patients with COVID-19: a key role for monocytes and macrophages. *Nat. Rev. Immunol.* **20**, 355–362 (2020).

5. Xu, Y. *et al.* Clinical Characteristics of SARS-CoV-2 Pneumonia Compared to Controls in Chinese Han Population. *medRxiv* 2020.03.08.20031658 (2020). doi:10.1101/2020.03.08.20031658

6. Azkur, A. K. *et al.* Immune response to SARS-CoV-2 and mechanisms of immunopathological changes in COVID-19. *Allergy* **75**, 1564–1581 (2020).

7. Gupta, A. *et al.* Extrapulmonary manifestations of COVID-19. *Nat. Med.* **26**, 1017–1032 (2020).

8. Rydyznski Moderbacher, C. *et al.* Antigen-Specific Adaptive Immunity to SARS-CoV-2 in Acute COVID-19 and Associations with Age and Disease Severity. *Cell* **183**, 996-1012.e19 (2020).

9. Handel, A., La Gruta, N. L. & Thomas, P. G. Simulation modelling for immunologists. *Nat. Rev. Immunol.* **20**, 186–195 (2020).

10. Sun, B. *et al.* Kinetics of SARS-CoV-2 specific IgM and IgG responses in COVID-19 patients. *Emerg. Microbes Infect.* **9**, 940–948 (2020).

11. Gonçalves, A. *et al.* Viral dynamic modeling of SARS-CoV-2 in non- human primates.

12. Du, S. Q. & Yuan, W. Mathematical modeling of interaction between innate and adaptive immune responses in COVID-19 and implications for viral pathogenesis. *J. Med. Virol.* **92**, 1615–1628 (2020).

13. Su, K., Ejima, K., Ito, Y., Iwanami, S. & Ohashi, H. Modelling SARS-CoV-2 Dynamics : Implications for Therapy. (2020).

14. Wang, S. *et al.* Modeling the viral dynamics of SARS-CoV-2 infection. *Math. Biosci.* **328**, 108438 (2020).

15. Gonçalves, A. *et al.* Timing of Antiviral Treatment Initiation is Critical to Reduce SARS-CoV-2 Viral Load. *CPT Pharmacometrics Syst. Pharmacol.* **9**, 509–514 (2020).

16. Tarek, M. & Savarino, A. Pharmacokinetic Basis of the Hydroxychloroquine Response in COVID-19: Implications for Therapy and Prevention. *Eur. J. Drug Metab. Pharmacokinet.* **45**, 715–723 (2020).

17. Goyal, A., Duke, E. R., Cardozo-Ojeda, E. F. & Schiffer, J. T. Mathematical modeling explains differential SARS CoV-2 kinetics in lung and nasal passages in remdesivir treated rhesus macaques. *bioRxiv* (2020). doi:10.1101/2020.06.21.163550

18. Iwanami, S. *et al.* Rethinking antiviral effects for COVID-19 in clinical studies: Early initiation is key to successful treatment. *medRxiv* (2020). doi:10.1101/2020.05.30.20118067

19. Czuppon, P. *et al.* Success of prophylactic antiviral therapy for SARS-CoV-2: Predicted critical efficacies and impact of different drug-specific mechanisms of action. *medRxiv* 1–24 (2020). doi:10.1101/2020.05.07.20092965

20. Goyal, A., Fabian, C. O. E. & Schiffer, J. T. Potency and timing of antiviral therapy as determinants of duration of SARS CoV-2 shedding and intensity of inflammatory response. *medRxiv* (2020). doi:10.1101/2020.04.10.20061325

21. Dobrovolny, H. M. Quantifying the effect of remdesivir in rhesus macaques infected with SARS-CoV-2. *Virology* **550**, 61–69 (2020).

22. Getz, M. *et al.* Rapid community-driven development of a SARS-CoV-2 tissue simulator. *bioRxiv* **2**, 1–28 (2020).

23. Sego, T. J. *et al.* A modular framework for multiscale, multicellular, spatiotemporal modeling of acute primary viral infection and immune response in epithelial tissues and its application to drug therapy timing and effectiveness. *PLoS Comput. Biol.* **16**, (2020).

24. Voutouri, C. *et al.* In silico dynamics of COVID-19 phenotypes for optimizing clinical management. *Proc. Natl. Acad. Sci. U. S. A.* **118**, (2021).

25. Bocharov, G., Volpert, V., Ludewig, B. & Meyerhans, A. Editorial: Mathematical Modeling of the Immune System in Homeostasis, Infection and Disease. *Front. Immunol.* **10**, 2019–2021 (2020).

26. She, Z.-S., Chen, X. & Hussain, F. Quantifying wall turbulence via a symmetry approach: a Lie group theory. *J. Fluid Mech.* **827**, 322–356 (2017).

27. Chen, X., Hussain, F. & She, Z.-S. Quantifying wall turbulence via a symmetry approach. Part 2. Reynolds stresses. *J. Fluid Mech.* **850**, 401–438 (2018).

28. Vetter, P. *et al.* Daily viral kinetics and innate and adaptive immune responses assessment in COVID-19: a case series. *medRxiv* 2020.07.02.20143271 (2020). doi:10.1101/2020.07.02.20143271

29. To, K. K. W. *et al.* Temporal profiles of viral load in posterior oropharyngeal saliva samples and serum antibody responses during infection by SARS-CoV-2: an observational cohort study. *Lancet Infect. Dis.* **20**, 565–574 (2020).

30. Tan, W. *et al.* Viral Kinetics and Antibody Responses in Patients with COVID-19. *medRxiv* 2020.03.24.20042382 (2020). doi:10.1101/2020.03.24.20042382

31. Lescure, F. X. *et al.* Clinical and virological data of the first cases of COVID-19 in Europe: a case series. *Lancet Infect. Dis.* **20**, 697–706 (2020).

32. Zhou, F. *et al.* Clinical course and risk factors for mortality of adult inpatients with COVID-19 in Wuhan, China: a retrospective cohort study. *Lancet* **395**, 1054–1062 (2020).

33. Chen, Y. & Li, L. SARS-CoV-2: virus dynamics and host response. *Lancet Infect. Dis.* **20**, 515–516 (2020).

34. Zhao, J. *et al.* Antibody Responses to SARS-CoV-2 in Patients With Novel Coronavirus Disease 2019. *Clin. Infect. Dis.* **71**, 2027–2034 (2020).

35. D'Alessio, F. R., Kurzhagen, J. T. & Rabb, H. Reparative T lymphocytes in organ injury. *J. Clin. Invest.* **129**, 2608–2618 (2019).

36. Chen, Z. & John Wherry, E. T cell responses in patients with COVID-19. *Nat. Rev. Immunol.* **20**, 529–536 (2020).

37. MacKinney, A. A. Effect of Aging on the Peripheral Blood Lymphocyte Count. *J. Gerontol.* **33**, 213–216 (1978).

38. Iwashyna, T. J. *et al.* Implications of Heterogeneity of Treatment Effect for Reporting and Analysis of Randomized Trials in Critical Care. *Am. J. Respir. Crit. Care Med.* **192**, 1045–1051 (2015).

39. Cheng, L. *et al.* Effect of Recombinant Human Granulocyte Colony–Stimulating Factor for Patients With Coronavirus Disease 2019 (COVID-19) and Lymphopenia. *JAMA Intern. Med.* (2020). doi:10.1001/jamainternmed.2020.5503

40. The State Council Information Office, P. R. of C. Press conference on the important role of traditional Chinese medicine in the prevention and treatment of COVID-19 and effective drugs. (2020). Available at: http://www.gov.cn/xinwen/2020-03/23/content_5494694.htm.

41. Black, D. S. & Slavich, G. M. Mindfulness meditation and the immune system: a systematic review of randomized controlled trials. *Ann. N. Y. Acad. Sci.* **1373**, 13–24 (2016).

42. Orme-Johnson, D. Medical care utilization and the transcendental meditation program. *Psychosom. Med.* **49**, 493–507 (1987).

43. Yan, L. & Wu, L. The effect of Taijiquan on the Human Body's T Lymphocyte Cells and Its Susset. *Wushu Res. public* (2007).

44. Chen, C., Wang, Y. & Li, J. Practicing JianshenqigongBaduanjin on drug addicts can reduce CD4+CD25+ regulatory T cells. *China J. Tradit. Chinese Med. Pharm.*

45. World Heath Organization: SARS-CoV-2 Variants. (2020). Available at: https://www.who.int/csr/don/31-december-2020-sars-cov2-variants/en/.

46. Mateus, J. *et al.* Selective and cross-reactive SARS-CoV-2 T cell epitopes in unexposed humans. *Science.* **370**, 89–94 (2020).

47. Marinaik, C. B. *et al.* Programming Multifaceted Pulmonary T Cell Immunity by Combination Adjuvants. *Cell reports. Med.* **1**, 100095 (2020).

48. Yan, L. *et al.* An interpretable mortality prediction model for COVID-19 patients. *Nat. Mach. Intell.* **2**, 283–288 (2020).

49. Liang, W. *et al.* Early triage of critically ill COVID-19 patients using deep learning. *Nat. Commun.* **11**, 1–7 (2020).

50. To, K. K.-W. *et al.* Temporal profiles of viral load in posterior oropharyngeal saliva samples and serum antibody responses during infection by SARS-CoV-2: an observational cohort study. *Lancet. Infect. Dis.* **20**, 565–574 (2020).

51. Pawelek, K. A. *et al.* Modeling within-host dynamics of influenza virus infection including immune responses. *PLoS Comput. Biol.* **8**, (2012).